Chemical Science

Accepted Manuscript

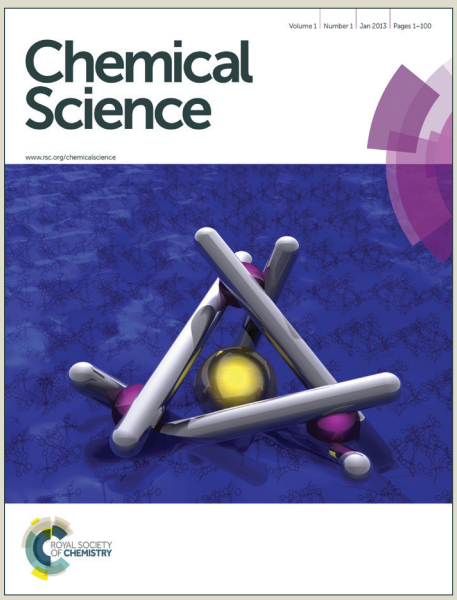

This is an *Accepted Manuscript*, which has been through the Royal Society of Chemistry peer review process and has been accepted for publication.

Accepted Manuscripts are published online shortly after acceptance, before technical editing, formatting and proof reading. Using this free service, authors can make their results available to the community, in citable form, before we publish the edited article. We will replace this *Accepted Manuscript* with the edited and formatted *Advance Article* as soon as it is available.

You can find more information about *Accepted Manuscripts* in the Information for Authors.

Please note that technical editing may introduce minor changes to the text and/or graphics, which may alter content. The journal's standard Terms & Conditions and the Ethical guidelines still apply. In no event shall the Royal Society of Chemistry be held responsible for any errors or omissions in this *Accepted Manuscript* or any consequences arising from the use of any information it contains.

ROYAL SOCIETY OF CHEMISTRY

www.rsc.org/chemicalscience

Cite this: DOI: 10.1039/c0xx00000x

www.rsc.org/xxxxxx

ARTICLE TYPE

A tripodal monopeptide ligand for asymmetric Rh(II) catalysis highlights unique features of on-bead catalyst development

Ramya Sambasivan,[a] Wenwei Zheng,[a] Scott J. Burya,[b] Brian V. Popp,[c] Claudia Turro,[b] Cecilia Clementi,[a] and Zachary T. Ball*[a]

Received (in XXX, XXX) Xth XXXXXXXXX 20XX, Accepted Xth XXXXXXXXX 20XX
DOI: 10.1039/b000000x

A tridentate eq-eq-ax peptide ligand for rhodium(II) complexes, discovered by high-throughput on-bead screening, is an efficient and selective catalyst for asymmetric cyclopropanation reactions. The metallopeptide catalyst is easily prepared and screened on bead. The axial imidazole ligand significantly improves catalyst function over previous *mono*-peptide Rh(II) catalysts. Experimental and theoretical investigations shed light on the role of the imidazole ligand and the structural consequences of imidazole ligation. These studies also explain the differential behavior of these metallopeptide catalysts in solution and on bead, and provide insight into the development of immobilized homogeneous catalysts in general.

Introduction:

Immobilized variants of soluble transition-metal complexes are an important class of catalysts that exist at the interface between the two other predominant metal catalysts: traditional heterogeneous materials and soluble, molecular transition-metal complexes. While immobilized catalysts have characteristics of both soluble and heterogeneous catalysts, they are typically discovered by adaptation from known soluble catalysts.[1] In this report, we describe efforts to identify immobilized rhodium(II) metallopeptide catalysts directly through screening on bead, and we present evidence of the unique opportunities available for the development of single-site, immobilized catalysts by conducting screens directly on immobilized species.

As roughly homogeneous molecular entities, immobilized catalysts exhibit single-site catalyst behavior and have ligand structures that can be readily altered and optimized. However, like heterogenous catalysts, these species resist catalyst contamination of the product, facilitate reaction workup and catalyst reuse, and can exhibit larger turnover numbers.[2] Immobilized catalysts have distinct requirements that differ from those of soluble catalysts. For example, homogeneous catalysts or ligands that act as higher-order assemblies or aggregates[3, 4] are not readily amenable to solid support, where site isolation behavior prevents assemblies and catalyst-catalyst interactions in general. On the other hand, catalyst-catalyst interactions are often detrimental to selective homogeneous catalysis, and can lead to catalyst-poisoning or decreased selectivity.[5] Ligand design often must prevent such interactions, e.g. through steric screening. Because of these disparate catalyst requirements, it is often true that soluble catalysts cannot be effectively adapted to immobilized settings. It is probably less appreciated, however, that many putative immobilized catalysts would be wholly unsuitable as soluble catalysts. This would imply that building immobilized catalysts by adapting soluble ones will prevent the discovery of many classes of successful immobilized structures.

As part of a program aimed at mimicking the properties of metalloenzymes[6-10] for developing asymmetric transition metal catalysts,[11-13] and for rhodium(II) carboxylate complexes in particular, we have demonstrated that peptides with two carboxylate side chains (glutamate or aspartate) serve as chelating ligands[12] for rhodium(II), allowing asymmetric catalytic reactions of diazo compounds.[14-17] Polypeptides are readily optimizable ligands for stereoselective catalysis owing to the chirality and structural variation present in amino acids.[18-20] Our initial efforts[14] developed screening methods that identified *bis*-peptide complexes of the type $Rh_2(peptide)_2$. In these initial efforts, we observed efficient chiral induction only for *bis*-peptide complexes. These complexes create a dense chiral environment near the two rhodium active sites, yet are difficult and inefficient to prepare: $Rh_2(peptide)_2$ complexes are formed as two isomers[16] with parallel and antiparallel orientations of the peptide ligands, which were separated by tedious RP-HPLC before use. In addition, as we have sought to develop more high-throughput, on-bead screening methods,[15] it was clear that $Rh_2(peptide)_2$ complexes could not be efficiently synthesized on solid support, so we resorted to screening solid-supported peptides as *mono*-peptide, $Rh_2(peptide)(OAc)_2$ complexes in 96-well format. The best sequences were then re-synthesized to make corresponding soluble $Rh_2(peptide)_2$ complexes. We successfully identified a number of useful *bis*-peptide complexes, but this roundabout approach relies on the expeditious—but uncertain—assumption that optimizing selectivity in $Rh_2(peptide)(OAc)_2$ complexes is a reasonable proxy for selectivity of $Rh_2(peptide)_2$ complexes. This approach was necessary because our initial screens of roughly 200 sequences did not uncover any *mono*-peptide complexes yielding the cyclopropane product in >55% ee.[15] However, monopeptide complexes, $Rh_2(peptide)(OAc)_2$ are attractive catalysts: they have lower molecular weight, comparing favorably

Chemical Science Accepted Manuscript

with traditional small-molecule catalysts. More importantly, because there is no isomer issue in their formation, they can be prepared in high yield, without wasting half of the catalyst preparation as the inferior isomer.

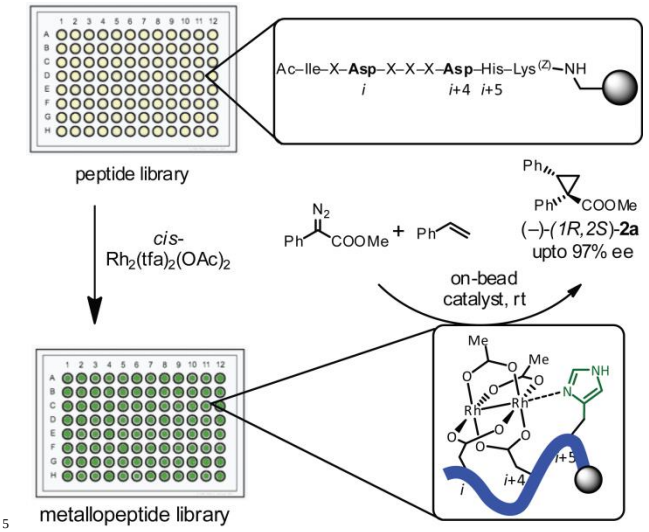

Fig. 1 On-bead screening of tripodal peptide ligands for cyclopropanation. Reaction conditions: diazo (6 µmol), styrene (60 µmol) and catalyst (~0.15 µmol), in CF_3CH_2OH, overnight at room temperature. All catalysts are attached to the resin at the C-terminus of the peptide, and the peptide N-terminus is acetylated.

When simple screening failed to uncover effective monopeptide catalysts, we decided to change course and modify our peptide design approach. The lack of symmetry of monopeptide complexes, Rh_2(peptide)$(OAc)_2$, implies that the two rhodium atoms should have different chemical environments; our modeling studies indicated that monopeptide complexes provided a robust chiral environment for only one of the two. One concept we explored was the potential for a third ligating residue that could bind to one axial position, potentially blocking the less selective catalytic site (Fig. 1, bottom right). Two recent reports indicate that external axial ligands can affect rhodium metallocarbene selectivity, and, intriguingly, both of these reports involve carboxylate ligands that create different chemical environments for the two Rh centers.[21,22,23] In one of these reports, we explored the addition of external phosphites and found modest increases in enantioselectivity.[21] Conceptually related efforts have examined catalysis with rhodium(II) complexes containing a dissociation-inert NHC ligand in an axial site.[24,25]

Incorporating a residue designed for axial ligation, such as histidine or methionine was a potentially more attractive means of accomplishing these same goals: it allows design control over which metal center is blocked by axial ligation, and it prevents the formation of catalytically dead *bis*-axial ligation. Furthermore, the intramolecular nature of such tris-chelating eq-eq-ax should minimize the involvement of "unbound" catalysts with two free axial sites. In this paper, we describe the development and exploration of such site-selective monopeptide catalysts affording high selectivities—up to 97% ee at room temperature (Fig. 1).

Results

Although straightforward in theory, creating tridentate ligands that feature a Lewis basic residue chelating to the axial site of rhodium(II) is experimentally challenging. In contrast to stable and largely covalent equatorial ligands, axial ligation is weak and readily reversible in aqueous solution (K_d ~50 µM).[26, 27] As a result, our experience has been that sequences with histidine or methionine residues, on complexation with Rh(II), form intermolecular axial interactions, resulting in ill-defined aggregates that are challenging to purify and isolate. Proper design of a peptide ligand that favors intramolecular axial interactions might potentially alleviate these issues, but on-bead catalyst preparation and screening should render these issues moot, since solid-supported peptides cannot engage in intermolecular interactions. We previously put into practice these ideas: a screen of several resin types and loadings found that so long as loading is kept low (~0.2 mmol/g), catalytic behavior on resins closely mirrored that in solution.[15, 17]

Table 1 High ee yielding sequences from Libraries 3,4 and 5 for the formation of product **2a**

ligand	ligand sequence	% ee[a]	% ee[b]
L2.36[15]	K^ZGDLANDMK^Z	51	–
L3.01	IGDLGNDHK^Z	56	–
L3.02	IGDNINDHK^Z	79	–
L3.03	K^ZGDQNNDHK^Z	56	–
L3.04	IGDQTNDHK^Z	68	–
L3.05	IGDLWNDHK^Z	71	–
L4.31	IGDNINDHK^Z	68	–
L4.28	IGDLFNDHK^Z	76	–
L4.46	IGDNG$^{t\text{-}Bu}$NDHK^Z	76	–
L4.49	IGDQWNDHK^Z	78	–
L4.52	IGDQYNDHK^Z	78	–
L5.60	IQDLTNDHK^Z	84	95
L5.64	IQDLG$^{t\text{-}Bu}$NDHK^Z	87	96
L5.66	IQDNG$^{t\text{-}Bu}$NDHK^Z	87	96
L5.67	IQDYG$^{t\text{-}Bu}$NDHK^Z	89	97
L5.75	IQDQWNDHK^Z	88	95
L5.78	IQDQYNDHK^Z	89	96

[a] Enantioselectivity of the crude product determined by chiral HPLC analysis. [b] Enantioselectivity of the pure isolated product determined by chiral HPLC analysis. $G^{t\text{-}Bu}$ = *tert*-butyl glycine;Z = benzyloxycarbonyl.

We designed and synthesized libraries to assess these ideas using a parallel synthesis approach in a 96-well-plate format previously developed in our group.[15] Starting with 9-mer peptide ligands with rhodium-binding aspartate residues at the 3rd and 7th residues, we chose for variation specific residues, based on modeling or the results of previous libraries. Variation was allowed with a group of two to eight structurally diverse amino acids. We synthesized 96 random members of the theoretical library (~5–10% of the possible sequences). Amino acid positions that were consistently seen in more selective catalysts were used to fix or heavily bias the next round of library screening. (for

Chemical Science Accepted Manuscript

complete details of the libraries and ee values, see SI). In this work, three 96-well libraries (L3, L4, and L5) were evolved sequentially from the previously reported L1 and L2.[15]

When we designed a 96-peptide random library (L3) that allowed incorporation of histidine and methionine in a subset of peptides, we found that the histidine- and methionine-containing peptides functioned as useful catalysts. Our earlier on-bead catalyst library (L2)[15] screening yielded a methionine-containing ligand, **L2.36** that afforded the product cyclopropane in 51% ee. Optimization of methionine-containing peptides was not fruitful, but switching to histidine as an axial-ligating residue resulted in a number of interesting catalysts. In L3 screen, five catalysts—all with histidine in the i+5 position—afforded cyclopropanation products in >55% ee (Table 1), higher than the selectivity observed with any of ~200 peptides in previous screens (L1 or L2).[15] Having found a preferred position for histidine incorporation, this residue was conserved predominantly in the i+5 position for L4 synthesis, which provided enantioselectivity up to 78%. A final library (library 5) incorporating histidine in the i+5 position and optimal amino acids from previous libraries in the other positions was synthesized. This library screen identified several on-bead monopeptide catalysts (**L5.xx**, see Table 1), varying only in the 4th or 5th amino acid, that each afforded the product in good (95–97%) enantioselectivity. Scrambling the histidine to other positions resulted in inferior catalysts.

Table 2 Asymmetric cyclopropanation with α-diazophenylacetate

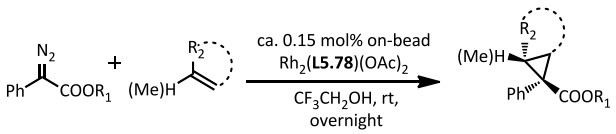

entry	alkene	R_1	R_2	prod.	ee (%)	yield
1		Me	Ph	**2a**	96	quant.[a]
2	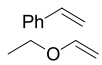	*t*Bu	Ph	**2b**	92	98%
3	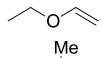	*t*Bu	OEt	**2c**	89	quant.[a]
4		*t*Bu	Ph	**2d**	99	quant.[a]
5	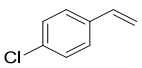	*t*Bu	(*p*-Cl)Ph	**2e**	95	quant.[a]
6	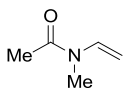	*t*Bu	NMeAc	**2f**	95[b]	92%[b]
7		*t*Bu	H	**2g**	94	quant.[a]

[a] Yield determined by NMR. [b] Reaction was carried out on a 1-mmol scale with respect to diazo substrate with Rh_2(**L5.67**)$(OAc)_2$ catalyst.

We tested this class of histidine-containing catalysts with various olefin substrates in cyclopropanation reactions with *tert*-butyl α-phenyldiazoacetate. Even at room temperature, >90% ee was observed with most olefins tested (Table 2), and in several cases was meaningfully higher than those achieved with the previous-generation bis-peptide catalysts. Notably, the reaction with a cyclic enol ether yielded the product cyclopropane in 94% ee (Table 2, entry 7) which is significantly greater than the selectivity observed with the solution-phase bis-peptide catalyst derived with the "winning" sequence identified via on-bead sceening in Library 2, published previously (80% ee, catalyst Rh_2(**L2.47**)$_2$-A).[15] We have successfully scaled up the cyclopropanation of an *N*-vinyl substrate up to 1 mmol without diminishment in yield or selectivity. Interestingly, and quite importantly, when we prepared catalysts in solution from purified peptides, significantly lower enantioselectivity was observed (81% vs. 37% ee for **L5.47**, see eqn 1). To test the impact of the key histidine residue, we made the catalyst with a His→Phe substitution. The nearly isosteric phenylalanine-containing catalyst (on bead) produced product in 59% ee (eq. 1).

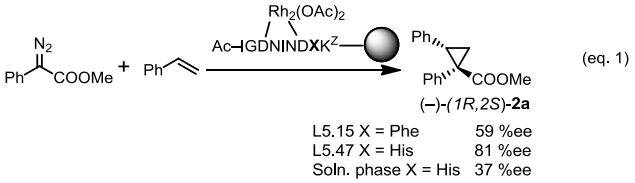

(eq. 1)

Discussion

The significantly better performance of the **L5.47** catalyst on bead, compared to its solution behavior, led us to examine the reasons for this difference. The catalyst **L5.47** contains two macrocycles formed upon tridentate binding to the rhodium center, a 12-membered ring and a 24-membered ring. This feature is somewhat unusual for transition-metal ligands. The majority of successful asymmetric ligands have small-ring chelates to the metal center. Strong catalyst preorganization, favoring chelate -structures, is common, especially in cases with larger, macrocyclic ring sizes formed upon metal binding. In solution, small-ring chelates and strong preorganization is important to prevent *bis*-metal binding leading to poorly organized aggregates.[28] In immobilized catalysts, this feature is less important. Because the site isolation afforded by solid support should generally limit the ability of a metal to bind two different ligands at once, preorganization should not be an important criterion for ligand design on solid support. This is especially true of relatively modest metal–ligand interactions, such as imidazole–rhodium coordination (K_d ~50 μM).

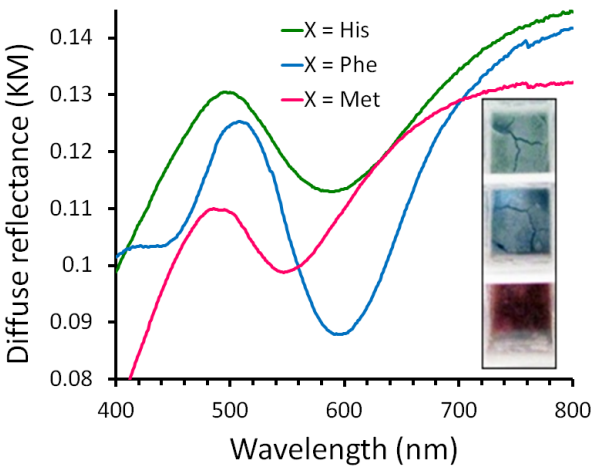

Fig. 2 Diffuse reflectance of the on-bead Rh_2(IGDNINDXK)$(OAc)_2$ catalysts in Kubelka Munk units (KM). Inset picture shows the wells with the on-bead catalyst. The λ @ lowest reflectance for X = His 590 nm; X = Phe 596 nm and X = Met 547 nm.

Chemical Science Accepted Manuscript

The poor enantioselectivity observed in solution with catalyst **L5.47** implies that a different catalyst structure acts in solution. The supported catalyst **L5.47** exhibits a clear blue-shift in visible absorbance, relative to the isosteric phenylalanine-containing catalyst, when measured by diffuse reflectance spectroscopy (Fig 2). A similar shift is observed with the related methionine-containing catalyst. The blue-shift is indicative of the presence of a strong donor ligand in the axial position. The blue-shift is visible to the naked eye as a color shift from blue to green (His) or pink (Met). We were able to validate the presence of axial imidazole–rhodium interactions through kinetic means as well. Within the dirhodium core, coordination of a strong donor ligand at one axial position is known to result in a decrease in reaction rate at the other rhodium atom, due to the electronic effect.[21, 23] Both histidine and methionine catalyst variants have significantly retarded reaction kinetics, with a k_{rel} that is 4- to 6-fold lower than the phenylalanine control, in line with previous work (Fig 3).[29]

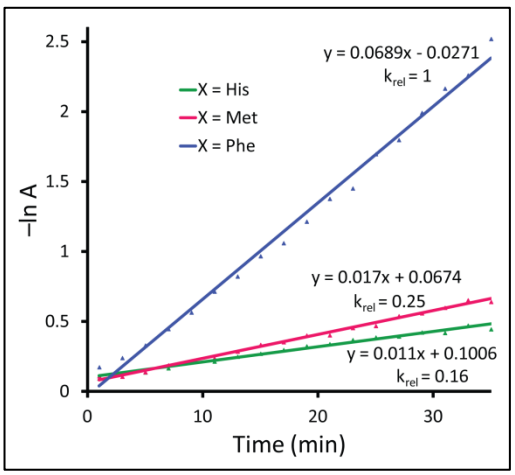

Fig. 3 Kinetics of the cyclopropanation of methyl α-phenyldiazoacetate and styrene at rt in CF_3CH_2OH catalyzed by on-bead Rh_2(IGDNIND**X**K)$(OAc)_2$.

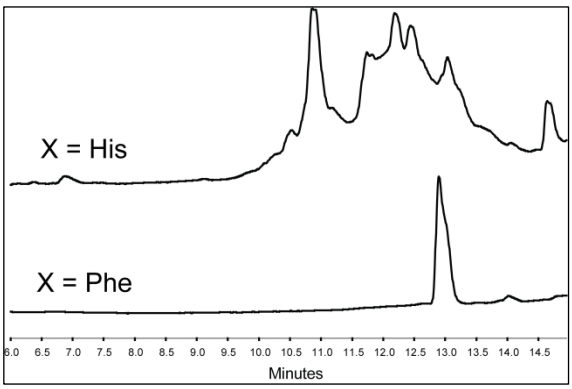

Fig. 4 HPLC traces of crude reaction mixture during solution-phase Rh_2(IGDNIND**X**K)$(OAc)_2$ synthesis.

The behavior in solution is significantly different. Both metallopeptides formed from His- or Phe-containing peptides are cleanly synthesized in high yield within three hours, as judged by analysis of the reaction mixture by MALDI–MS (see SI), which ionization conditions generally break up aggregates. While the Phe-containing peptide exhibits an expected HPLC with a single major peak (Fig. 4, X=Phe), the chromatogram for the histidine peptide (X=His) shows a large number of broad, overlapping peaks, indicative of aggregate formation through intermolecular imidazole interactions. We have observed this aggregation phenomenon previously when synthesizing rhodium variants of biologically relevant peptides, a problem solved by substituting for natural methionine and histidine residues.[30]

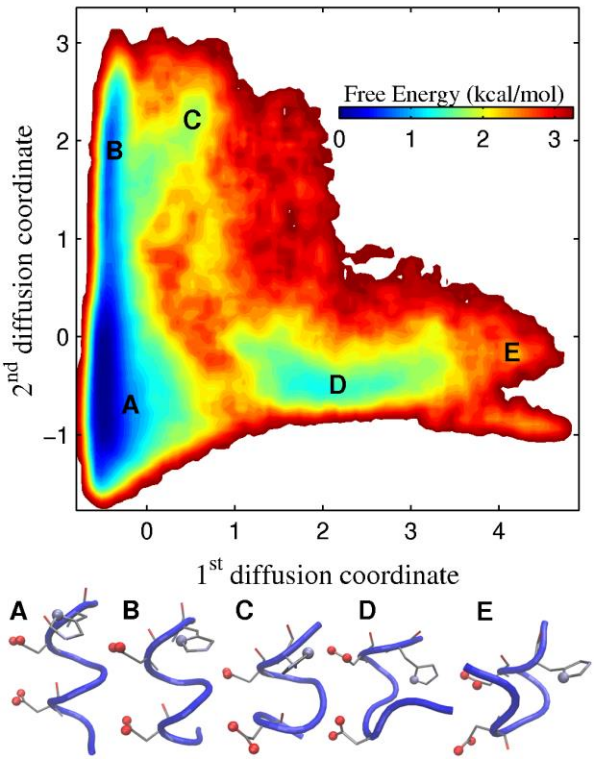

Fig. 5 Upper panel: Free energy as a function of the first and second diffusion coordinates with minima marked; Lower panel: The typical configurations in the free energy minima marked in the upper panel.

To understand how histidine coordination affects catalyst selectivity, we conducted a computational study. Molecular Dynamics (MD) calculations were performed in conjunction with quantum mechanical modeling using Density Functional Theory (DFT). The former helps to identify stable peptide-binding configurations, whereas the latter provides an accurate structure of the transition metal complex. The sequence IGDNINDHK was chosen as the model system for MD simulations. The peptide was simulated in implicit solvent with Generalized Born formalism in GROMACS v4.5.4.[31] A total of 18 simulations (each 500 ns long) were performed and the data was recorded every 100 ps. The free energy profile and stable states of the free peptide were identified by applying LSDMap and analyzing the merged data (90,000 frames) from these simulations. LSDMap is a recently developed nonlinear dimensionality reduction method[32] to define 'optimal' reaction coordinates, that correspond to the slowest collective motions of the system, and extract them from MD simulation. The free energy projected onto the first two diffusion coordinates from the LSDMap calculation is shown in Figure 5.

The MD simulations of the free peptide identify α-helix-like structures (Fig 5, states A, B, C) to be predominant in solution.

Chemical Science Accepted Manuscript

We have previously demonstrated that chelating a rhodium(II) center to carboxylate side chains with *i*, *i*+4 spacing (as employed here) significantly increases this bias in favor of α-helix structures. Thus, it is reasonable to assume that the simple bis-carboxylate peptides adopt a helical structure when bound to rhodium, in line with previous data and assumptions. The MD simulations indicate that non-helical structures (states D,E; random or turn-like structures) account for only a small part of the available energy landscape. The helical structures constitute nearly 86% of the total number of frames calculated. To understand the impact of imidazole coordination, we identified conformations from each state found in MD simulations that placed the carboxylate and histidine residues closest to the positions necessary for optimal rhodium-binding geometry. The chosen conformations were then subjected to steered MD in GROMACS v4.5.4 with PLUMED plug-in.[33] A total of 22 conformations were identified that had the appropriate binding angles to the arbitrary dirhodium core. Importantly, regardless of the initial conformation, all computed tridentate metallopeptides exhibited similar non-helical, turn-like structure. Further refinement of the optimal tridentate metallopeptide structure was achieved using DFT methods (see SI for details), providing a reasonable and representative structure of tridentate catalysts (Fig. 6b).

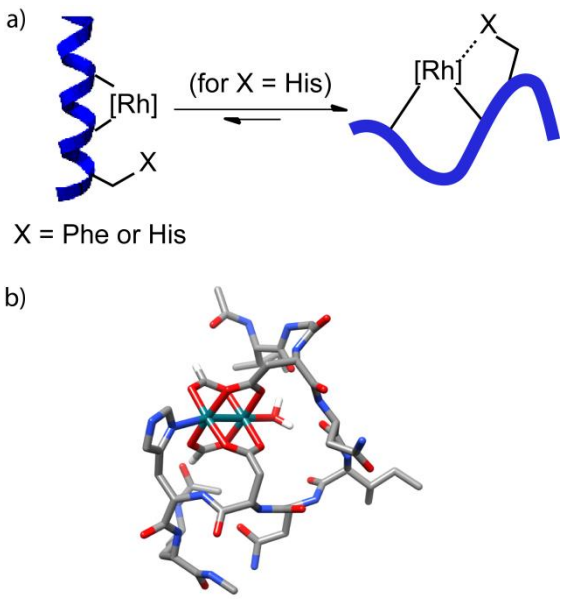

Fig. 6 (a) Cartoon depiction of preferred secondary structure attained upon Rh(II) complexation. Left: peptide IGDNINDFK attains an α helix; Right: peptide IGDNINDHK is proposed to attain a hairpin turn (b) DFT energy minimized model of the Rh_2(IGDNINDHK)$(OAc)_2$ catalyst featuring axial imidazole ligation. The putative catalytic site *trans* to the axial-imidazole ligand was occupied by a molecule of water. For simplicity, formates were used instead of acetates. Hydrogen atoms have been omitted for clarity.

The computational results demonstrate that the third ligand (imidazole) causes a structural switch—from helical to turn-like—of the peptide backbone (Fig. 6a). The helical structure is completely inaccessible when the imidazole group is bound to the axial position. The fact that the ligand itself prefers helical conformations may explain the complex behavior of the catalyst in solution: histidine coordination comes at the cost of disrupting the preferred helical secondary structure. Thus, in solution, intermolecular histidine–rhodium interactions, which do not require disrupting the helical conformation, out-compete intramolecular interactions; on bead, intermolecular interactions are not possible.

Conclusions:

This tripodal class of peptide-based ligands allows construction of monopeptide catalysts of the type Rh_2(peptide)$(OAc)_2$, a significant step forward relative to previous, soluble *bis*-peptide Rh_2(peptide)$_2$ catalysts. In addition to improved enantioselectivity in cyclopropanation reactions, these immobilized catalysts are trivial to prepare. Standard on-bead peptide synthesis and rhodium metalation methods deliver active catalysts with no purification beyond simple filtration. In contrast, our previous *bis*-peptide catalysts Rh_2(peptide)$_2$ required careful HPLC separation of orientational (parallel and antiparallel) isomers, wasting half of the material and making the catalysts inappropriate for preparative work. The catalysts are selective at room temperature, unlike previous soluble bis-peptide catalysts that required cryogenic conditions for selectivity, and immobilized metallopeptide catalysts can be easily separated by filtration. These advances are all made possible by the power of on-bead catalyst discovery, which enable us to synthesize and assess catalysts in 96-well plate format in a matter of days.

Work in metallopeptide design and catalysis is often motivated by the inspiration of natural metalloenzymes. Metalloenzymes use large polypeptide structure to provide steric screening and to control access to the active site, resulting in largely site-isolated active sites. Minimalist peptide ligands are rarely able to replicate this aspect of natural enzymes. Our data suggest that by employing an on-bead strategy, we are able to build enzyme-like site isolation into a metallopeptide catalyst, avoiding destructive intermolecular interactions in the process. Together with modern analytical tools that can assess structure of solid-supported materials, it is possible that metalloenzyme design fields would benefit from increased use of immobilized platforms for catalyst development.

This work represents the first use of an axial-binding component in ligand design to control rhodium(II) diazo chemistry. This result opens up new possibilities for ligand design, in contrast to a previous report that concluded that one axial ligand results in an inactive catalyst. Computational modelling suggests that the presence of the key histidine residue orchestrates a switch from helix to turn-like structure upon binding to the rhodium core. This approach would not have been possible in solution, where intermolecular histidine interactions conspire to result in ill-defined, nonselective aggregates. Immobilized ligand discovery facilitates ligand screening, but also allows the discovery of selective chelating ligands, under site-isolated conditions, that suffer from competing aggregation or other intermolecular interactions in solution. Ligand classes involving macrocyclic chelates or lacking strong preorganization might be especially amenable to this type of an immobilized catalyst discovery approach.

Acknowledgements:

Chemical Science Accepted Manuscript

We thank Prof. Angel Marti and Avishek Saha for assistance with diffuse reflectance measurements. We acknowledge financial and computing resources from West Virginia University (B.V.P.) and financial support from the Robert A. Welch Foundation Research Grant C-1680 (Z.T.B.) and Research Grant C-1570 (C.C.). This work was supported by the National Science Foundation under grant numbers CHE-1055569 (Z.T.B.), CHE-1152344 (C.C.) and CHE-1265929 (C.C.). C.T. acknowledges partial support of this work by the Chemical Sciences, Geosciences and Biosciences Division, Office of Basic Energy Sciences, Office of Science, U.S. Department of Energy (Grant No. DE-FG02-13ER16423).

Notes and references

[a] *Department of Chemistry, Rice University, MS 60, 6100 Main street, Houston, Texas, USA. Fax: 713 348 5155; Tel: 713 348 6159; E-mail: zb1@rice.edu*

[b] *Department of Chemistry and Biochemistry, The Ohio State University, Columbus, Ohio, USA Tel: 614 292 6708; E-mail: turro@chemistry.ohio-state.edu*

[c] *Bennett Department of Chemistry, 100, Prospect street, Morgantown, West Virginia, USA. Fax: 304 293 4904; Tel: 304 293 0773; E-mail: brian.popp@mail.wvu.edu*

†Electronic supplementary information (ESI) available: Experimental details, library results, characterization data for cyclopropane products, MD and DFT refinement data. See DOI: 10.1039/b000000x/

1. I. F. J. Vankelecom and P. A. Jacobs, in *Chiral Catalyst Immobilization and Recycling*, Wiley-VCH Verlag GmbH, 2007, pp. 19-42.
2. Z. Wang, K. Ding and Y. Uozumi, in *Handbook of Asymmetric Heterogeneous Catalysis*, Wiley-VCH Verlag GmbH & Co. KGaA, 2008, pp. 1-24.
3. P. Mastrorilli and C. F. Nobile, *Coord. Chem. Rev.*, 2004, **248**, 377-395.
4. D. Castellnou, M. Fontes, C. Jimeno, D. Font, L. Solà, X. Verdaguer and M. A. Pericàs, *Tetrahedron*, 2005, **61**, 12111-12120.
5. S. H. Hong, A. G. Wenzel, T. T. Salguero, M. W. Day and R. H. Grubbs, *J. Am. Chem. Soc.*, 2007, **129**, 7961-7968.
6. P. J. Deuss, R. den Heeten, W. Laan and P. C. Kamer, *Chemistry*, 2011, **17**, 4680-4698.
7. F. Rosati and G. Roelfes, *ChemCatChem*, 2010, **2**, 916-927.
8. C. M. Thomas and T. R. Ward, *Chem. Soc. Rev.*, 2005, **34**, 337-346.
9. J. Steinreiber and T. R. Ward, *Coord. Chem. Rev.*, 2008, **252**, 751-766.
10. T. R. Ward, *Acc. Chem. Res.*, 2010, **44**, 47-57.
11. A. Mori, H. Abet and S. Inoue, *Appl. Organomet. Chem.*, 1995, **9**, 189-197.
12. Z. T. Ball, *Acc. Chem. Res.*, 2012, **46**, 560-570.
13. P. J. Deuss, R. den Heeten, W. Laan and P. C. J. Kamer, *Chem. Eur. J.*, 2011, **17**, 4680-4698.
14. R. Sambasivan and Z. T. Ball, *J. Am. Chem. Soc.*, 2010, **132**, 9289-9291.
15. R. Sambasivan and Z. T. Ball, *Angew. Chem. Int. Ed.*, 2012, **51**, 8568-8572.
16. R. Sambasivan and Z. T. Ball, *Org. Biomol. Chem.*, 2012, **10**, 8203-8206.
17. R. Sambasivan and Z. T. Ball, *Chirality*, 2013, **25**, 493-497.
18. P. Krattiger, R. Kovasy, J. D. Revell, S. Ivan and H. Wennemers, *Org. Lett.*, 2005, **7**, 1101-1103.
19. J. D. Revell, D. Gantenbein, P. Krattiger and H. Wennemers, *Biopolymers*, 2006, **84**, 105-113.
20. M. Wiesner, J. D. Revell and H. Wennemers, *Angew. Chem. Int. Ed.*, 2008, **47**, 1871-1874.
21. A. N. Zaykov and Z. T. Ball, *Tetrahedron*, 2011, **67**, 4397-4401.
22. V. N. G. Lindsay, C. Nicolas and A. B. Charette, *J. Am. Chem. Soc.*, 2011, **133**, 8972-8981.
23. For a contradictory analysis of axial ligands in rhodium metallocarbene chemistry, see: M. C. Pirrung, H. Liu and A. T. Morehead, *J. Am. Chem. Soc.*, 2002, **124**, 1014-1023.
24. A. F. Trindade, J. A. S. Coelho, C. A. M. Afonso, L. F. Veiros and P. M. P. Gois, *ACS Catalysis*, 2012, **2**, 370-383.
25. P. M. P. Gois, A. F. Trindade, L. F. Veiros, V. André, M. T. Duarte, C. A. M. Afonso, S. Caddick and F. G. N. Cloke, *Angew. Chem. Int. Ed.*, 2007, **46**, 5750-5753.
26. A. M. Dennis, R. A. Howard and J. L. Bear, *Inorg. Chim. Acta*, 1982, **66**, L31-L34.
27. K. Das and J. L. Bear, *Inorg. Chem.*, 1976, **15**, 2093-2095.
28. B. M. Trost and R. W. Warner, *J. Am. Chem. Soc.*, 1982, **104**, 6112-6114.
29. M. C. Pirrung and A. T. Morehead, *J. Am. Chem. Soc.*, 1996, **118**, 8162-8163.
30. B. V. Popp and Z. T. Ball, *Chem. Sci.*, 2011, **2**, 690-695.
31. B. Hess, C. Kutzner, D. van der Spoel and E. Lindahl, *J. Chem. Theory Comput.*, 2008, **4**, 435-447.
32. M. A. Rohrdanz, W. Zheng, M. Maggioni and C. Clementi, *J. Chem. Phys.*, 2011, **134**, 124116-124111.
33. M. Bonomi, D. Branduardi, G. Bussi, C. Camilloni, D. Provasi, P. Raiteri, D. Donadio, F. Marinelli, F. Pietrucci, R. A. Broglia and M. Parrinello, *Comput. Phys. Commun.*, 2009, **180**, 1961-1972.

Chemical Science Accepted Manuscript